Electrochimica Acta 141 (2014) 82–88

Contents lists available at ScienceDirect

Electrochimica Acta

journal homepage: www.elsevier.com/locate/electacta

A simple, rapid and green method based on pulsed potentiostatic electrodeposition of reduced graphene oxide on glass carbon electrode for sensitive voltammetric detection of sophoridine

Fei Wang[a], Yanju Wu[a,b], Kui Lu[a,*], Lin Gao[a], Baoxian Ye[b,**]

[a] Department of Material and Chemistry Engineering, Henan Institute of Engineering, Zhengzhou, 450007, P. R. China
[b] Department of Chemistry, Zhengzhou University, Zhengzhou, 450001, P. R. China

ARTICLE INFO

Article history:
Received 18 April 2014
Received in revised form 22 May 2014
Accepted 2 July 2014
Available online 17 July 2014

Keywords:
Reduction of graphene oxide
Pulse potentiostatic method
Voltammetric sensor
Sophoridine

ABSTRACT

A simple, rapid and green method was described for sensitive voltammetric detection of sophoridine based on graphene nanosheets directly deposited onto a glassy carbon electrode (GCE) by pulsed potentiostatic reduction of a graphene oxide (GO) colloidal solution. The resulting electrodes (PP-ERGO/GCE) were characterized by electrochemical methods and scanning electron microscopy. Moreover, the electrochemical behaviors of sophoridine at the modified electrode were investigated in detail by cyclic voltammetry (CV), chronoamperometry (CA) and chronocoulometry (CC). Compared with the bare GCE and the preparation of reduced graphene oxide (RGO) films by potentiostatic method (PM) modified GCE, PP-ERGO/GCE could intensively enhance the oxidation peak currents and decrease the overpotential of sophoridine. Under the selected conditions, the modified electrode showed a linear voltammetric response to sophoridine within the concentration range of $8.0 \times 10^{-7} \sim 1.0 \times 10^{-4}$ mol L^{-1} [1], with the detection limit of 2.0×10^{-7} mol L^{-1}. And, the method was also applied to detect sophoridine in spiked human urine with wonderful satisfactory.

1. Introduction

Sophoridine, a quinolizidine alkaloid, is a main active ingredient of kinds of Sophora plants in traditional Chinese herbal drug [1]. The studies of pharmacological effect have shown that sophoridine has wide pharmacological effects including anti-arrhythmic [2], antiviral effects [3] and immunological enhancement [4]. And, it also exhibits the potential therapeutic efficacy in malignant tumors in the digestive tract such as colorectal carcinoma, gastric cancer, and esophageal cancer [5,6]. Accordingly, accurate analytical method for sophoridine is necessary and some determination techniques have been developed, such as high performance liquid chromatography (HPLC) [7,8], gas chromatography–mass spectrometer (GC-MS) [9], nonaqueous capillary electrophoresis (CE) [10] and electrogenerated chemiluminescence (ECL) [11]. But, some of them are time-consuming, expensive or involve a tedious extraction process before detection. In contrast, electrochemical method is simple, rapid, sensitive and inexpensive. Furthermore, the redox properties of drugs can provide insight into their metabolic fate, their in vivo redox processes, and their pharmacological activity [12]. Recently, the report regarding the voltammetric and amperometric determination of sophoridine is raised [13,14], but very limited.

In the past decades, several forms of carbon materials (e.g. ordered mesoporous carbon [15], carbon nanofiber [16], carbon nanotube [17]) have been studied to use for developing electrochemical sensors. Graphene, a perfect two-dimensional carbon material found in 2004 [18,19], is an ideal material for electrochemistry [20] because of its very large 2D electrical conductivity, large surface area and low cost. At present, graphene is usually prepared in large quantities by a chemical method [21] or an electrochemical reduction [22] of graphene oxide (GO). A series of investigations showed that chemically reduced graphene oxide (CRGO) always needs excessive reducing agents, and additionally some oxygenated species cannot be completely reduced by chemical treatment, which may degrade the electrochemical performance. As compared with the chemical method, electrochemical reduction provides several advantages, including being simple, rapid, green and efficient [23–26]. More importantly, the

* Corresponding author. Department of Material and Chemistry Engineering, Henan Institute of Engineering, Zhengzhou, 450007, P. R. China.
Tel.: +86 0371 67718925, fax: +86 0371 67718909.
** Corresponding author. Department of Chemistry, Zhengzhou University, Zhengzhou, 450001, P. R. China. Tel.: +86 0371 67781757, Fax: +86 0371 67763654.
E-mail addresses: luckyluke@haue.edu.cn (K. Lu), yebx@zzu.edu.cn (B. Ye).

http://dx.doi.org/10.1016/j.electacta.2014.07.018
0013-4686/

highly negative potential used in the electrochemical reduction of graphene oxide (ERGO) efficiently reduces the oxygen-containing functional groups [27]. Recently, the synthesis and applications of ERGO as electrochemical sensors [28–30], biosensors [31], and supercapacitors [32] have attracted considerable interest because of its unique properties. The ERGO has usually been obtained by two steps: (1) drop-casting of graphene oxide solution on basal electrodes; (2) then, electrochemical reduction of above modified electrodes. And, a series of electrochemical methods, such as cyclic voltammetry (CV) [28,30–32] and potentiostatic method [29], has been employed. However, the pulse potentiostatic method (PPM) [33], having advantages, including simplicity, time savings and high purity of the deposits, has little been adopted in the ERGO field.

In this work, an ERGO film was prepared onto the glassy carbon electrode (GCE) directly from GO dispersions by PPM, and the resulting electrode was used to determine sophoridine. The electrochemical behaviors of sophoridine at the modified electrode were investigated in detail by cyclic voltammetry (CV), chronoamperometry (CA) and chronocoulometry (CC). Compared with the bare GCE and the preparation of reduced graphene oxide (RGO) films by PM modified GCE, the modified electrode could intensively enhance the oxidation peak currents and decrease the overpotential of sophoridine. In addition, oxidation peak currents were found to be sensitively responding to the sophoridine, and a linear voltammetric response to sophoridine within the concentration range of $8.0 \times 10^{-7} \sim 1.0 \times 10^{-4}$ mol L^{-1} was obtained under the selected conditions. Based on these results, we believe it is a simple, rapid, green and promising method for determination of sophoridine. And, this work would enlarge the application range of graphene in electroanalytical chemistry.

2. Experimental

2.1. Apparatus and Reagents

Model CHI 650A electrochemical system (CHI Instrumental, Shanghai, China) and RST5000 electrochemical workstation (Zhengzhou Shiruisi Instrument Co., Ltd., Zhengzhou, China) were employed for electrochemical techniques. Atomic Force Microscopy (AFM) images were obtained with a BenYuan CSPM-5500 atomic force microscopy (Guangzhou BenYuan nanometer Instrument Co., Ltd., Guangzhou, China). Scanning electron microscopy (SEM) images were obtained with a Quonxe-2000 field emission scanning electron microscope (FEI Company, Holland). A standard three-electrode electrochemical cell was used with glassy carbon electrode (d = 3 mm) or modified GCE as working electrode, platinum (Pt) wire as auxiliary electrode and a saturated calomel electrode (SCE) as reference electrode (the internal solution was saturated KCl solution). All the pH measurements were made with a PHS-3 C precision pH meter (Leici Devices Factory of Shanghai, China), which was calibrated with standard buffer solution at 25 ± 0.1 °C every day.

All reagents were of analytical grade and were used as received. Double distilled water was used for all preparations. Sophoridine was purchased from National Institute for the Control of Pharmaceutical and Biological Products (Beijing, China). Stock solution (2.0×10^{-3} mol L^{-1}) of sophoridine was prepared with doubly distilled water and stored at 4°C in the dark.

2.2. Preparation of the modified electrode

Firstly, GO was synthesized from graphite by the modified Hummers method [34]. The exfoliated GO was obtained by ultrasound of the GO dispersion, and centrifugating at 3000 rpm for 15 min. The resulting GO deposited on the mica were characterized by AFM. The results revealed that the GO sheets were almost single-layer, see Fig. S1. And the average thickness of single-layer GO sheets was approximately 1 nm.

Prior to modification, the bare GCE was polished successively with 0.3 and 0.05 μm Al_2O_3 power and rinsed thoroughly with doubly distilled water between each polishing step. After that, the GCE was sonicated in ethanol and doubly distilled water each for 2 min, and dried under N_2 blowing. After that, the bare GCE was immersed in pH 6.0 phosphate buffer solutions (PBS) containing 0.8 mg mL^{-1} GO, and prepared for electrodepositing by PPM under constant stirring. The optimal parameters of electrodeposition were listed as follows: upper limit potential E_a, 0.1 V; lower limit potential E_c, -1.2 V; anodic pulse duration t_a, 0.6 s; cathodic pulse duration t_c, 0.3 s; experimental time t_{exp}, 180 s. The overall reduction time (t_{re}) can be calculated from the following equation: $t_{re} = t_{exp} \times t_c/(t_c + t_a)$. The optimal parameters of electrodeposition (t_a, t_c and t_{re}) were described in the S1. The obtained electrode was denoted as PP-ERGO/GCE. For comparison, the ERGO/GCE was also fabricated with the similar procedure by the potentiostatic method (PM).

2.3. Analysis of spiked urine samples

The urine samples were drawn from healthy individuals immediately before the experiments. Spiked urine samples were obtained by treating 1.0 mL aliquots of urine with appropriate amount of sophoridine standard solutions. A 20 μL aliquot of spiked urine was diluted with 10 mL 0.2 mol L^{-1} pH = 7.5 phosphate buffer solutions (PBS), without any pre-treatment, and transferred into the voltammetric cell. The SWV was recorded to achieve the quantitative analysis (with a scan increment of 4 mV, pulse amplitude of 30 mV, and pulse frequency of 25 Hz).

3. Results and Discussion

3.1. Pulsed potentiostatic electrodeposition of RGO film on GCE

As applying a positive potential, GO sheets could be deposited on the electrode; because GO colloids exhibit negative charges in weak acid [35]. According to the literature [30], the as-deposited GO sheets can be electrochemically reduced at E = -1.1 V *vs* SCE. Here, we use the PPM to achieve the electrodeposition of RGO films, in which 0.1 V *vs* SCE is used to deposit GO sheets on GCE, followed by applying -1.2 V *vs* SCE to electrochemically reduce the as-deposited GO sheets to RGO sheets.

To illustrate the pulse procedure used for the ERGO film, the evolution in time of the E and the i for the process of PM and PPM was investigated, see Fig. 1. When the E is constant and uninterrupted (see the inset of Fig. 1A), the i decays quickly as soon as the potential is imposed, probably due to the change in the precursor's concentration when the GO sheets close the electrode surface start to react. Later, the i attains a limiting value (see Fig. 1A), typical of a deposition process controlled by mass transport. The i-t response is altered when the E is pulsed (see the inset of Fig. 1B). After the potential E_c is applied, the i increases sharply and then decreases tending to a steady value as in potentiostatic mode (see Fig. 1B). As potential E_a is imposed, the i drops sharply, reaching values close to zero. This is a so-called "relaxation period" that allows the diffusion of GO sheets to areas where they have been quickly consumed while applying E_a. When a new pulse start, the distribution of GO sheets on the electrode surface is supposed to be more homogenous [36]. Therefore, the PPM can gain more uniform the thin films.

3.2. Morphological characterization of the PP-ERGO/GCE

To obtain further information on the successful preparation of RGO films by PPM and illustrate the difference of electrochemical

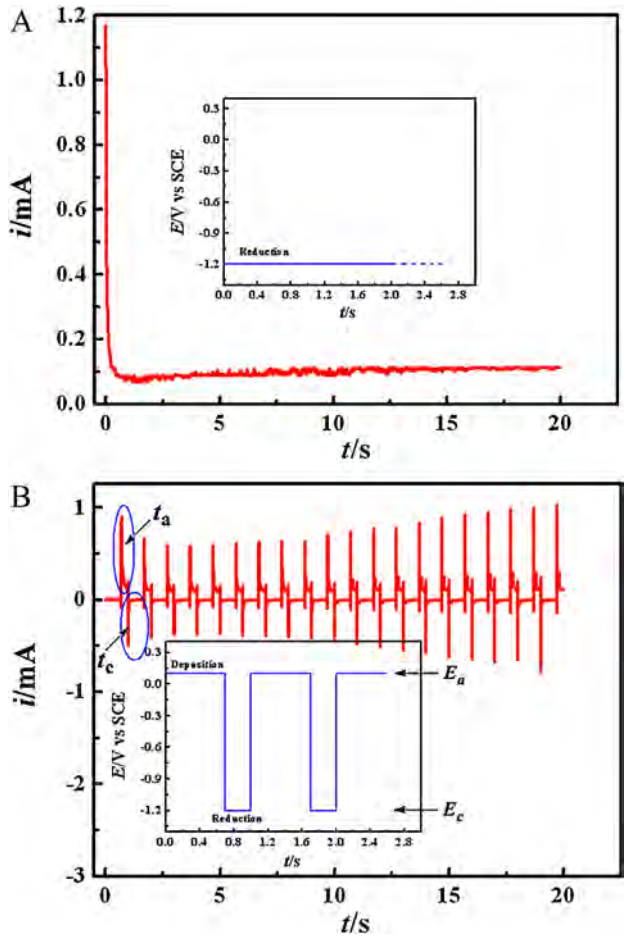

Fig. 1. Characteristic *i*–t response registered for potentiostatic (A) and pulsed electrodeposition (B). The inset in each figure outlines the *E*–t profile imposed for each method, during the electrodeposition of RGO films.AFM image of GO from its dilute aqueous dispersion on freshly cleaned mica.

properties, morphologies of the ERGO/GCE (Fig. 2A) and PP-ERGO/GCE (Fig. 2B) were characterized by using SEM. As showed in Fig. 2A, the preparation of RGO films by PM modified GCE showed a loose, disorder and stacked surface. In contrast, preparation of RGO films by PPM display closely associated with each other to form thin and crumpled sheets, and the edges of individual sheets were distinguishable with kinked and wrinkled areas (Fig. 2B), which is highly beneficial in maintaining a high surface area on the electrode and helpful in constructing an interface for the electrochemical sensors. Moreover, the films barely show aggregation, indicating that the assembly of RGO films by PPM on a solid substrate is a good way to prevent the aggregation of RGO.

3.3. Electrochemical characterization of the PP-ERGO/GCE

In order to highlight the particular feature of the proposed electrode, its voltammetric response for redox probe $[Fe(CN)_6]^{3-/4-}$ was compared with another electrode. Fig. 3 shows the cyclic voltammograms (CVs) of bare GCE (curve a), ERGO/GCE (curve b) and PP-ERGO/GCE (curve c) in 1.0×10^{-3} mol L^{-1} $K_3[Fe(CN)_6] + 0.1$ mol L^{-1} KCl solution. A pair of redox peaks of $[Fe(CN)_6]^{3-/4-}$ is showed on bare GCE with the peak-to-peak separation (ΔE_p) as 86 mV at the scan rate of 100 mV s^{-1}. While on ERGO/GCE, both cathodic and anodic peak currents increase obviously with the ΔE_p value decrease to 71 mV. The largest peak currents and the smallest ΔE_p of redox probe $Fe(CN)_6^{3-/4-}$ is observed on PP-ERGO/GCE. The results suggested that the properties of the ERGO films prepared by

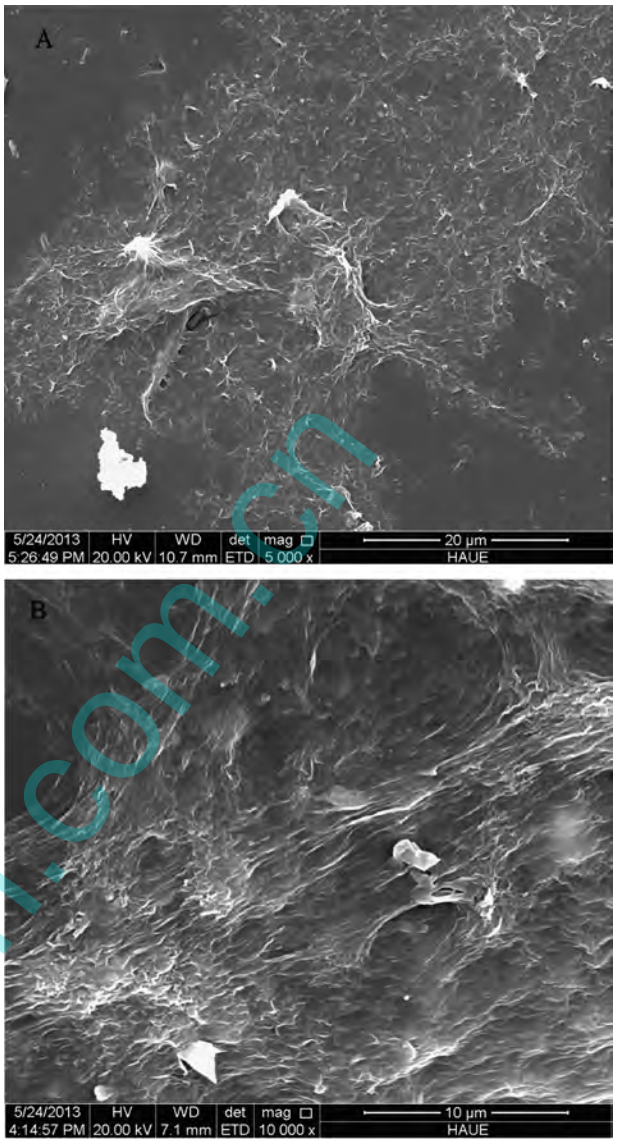

Fig. 2. The SEM images obtained from the ERGO/GCE (A) and PP-ERGO/GCE (B).

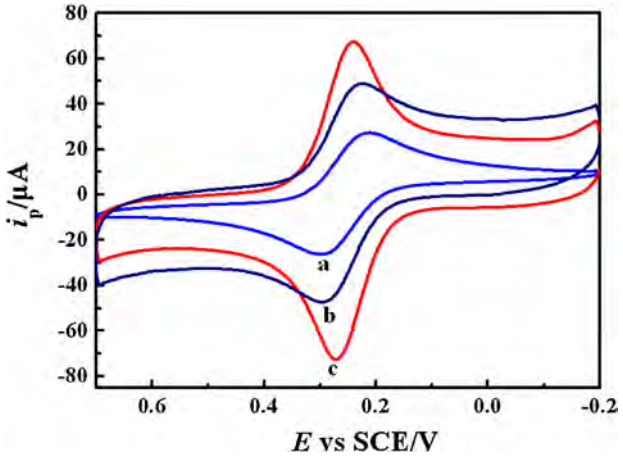

Fig. 3. CVs of a bare GCE (curve a), ERGO/GCE (curve b) and PP-ERGO/GCE (curve c) in 1.0×10^{-3} mol L^{-1} $K_3[Fe(CN)_6] + 0.1$ mol L^{-1} KCl solution.

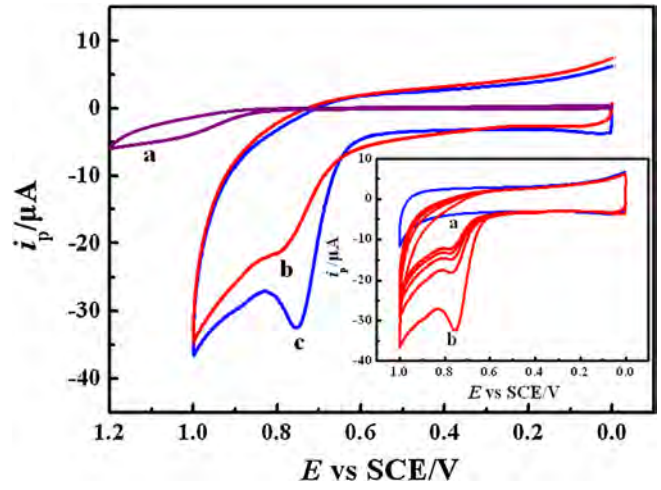

Fig. 4. CVs of 1.0×10^{-4} mol L^{-1} sophoridine at a bare GCE (curve a), ERGO/GCE (curve b) and PP-ERGO/GCE (curve c) in 0.2 mol L^{-1} PBS (pH = 7.5), ν = 0.05 V s^{-1}; CVs of the background (curve a) and successive CVs of sophoridine (1.0×10^{-4} mol L^{-1}, curve b) at the PP-ERGO/GCE in the inset.

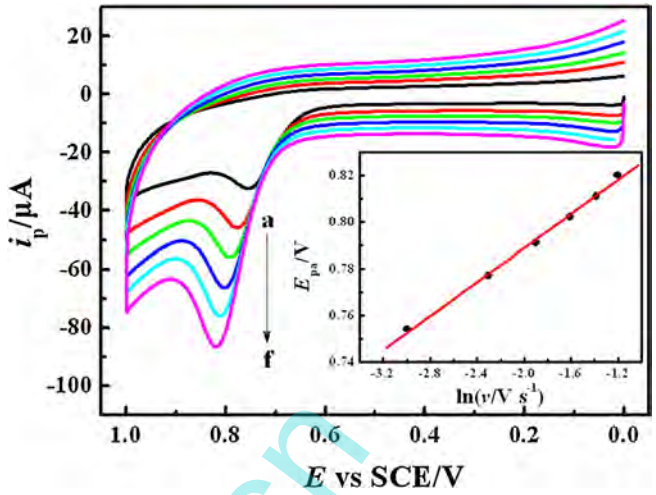

Fig. 5. CVs of 1.0×10^{-4} mol L^{-1} sophoridine at the PP-ERGO/GCE at different scan rate (from 1 to 6: 0.05, 0.10, 0.15, 0.20, 0.25, 0.30 V s^{-1}); insets show the relationship of the peak potential E_{pa} against ln ν, the other experimental conditions are the same as those described in Fig. 6.

PPM in increasing the active surface area of electrode and accelerating the electron transfer rate was superior to that of PM. Moreover, we found also that the redox peaks current are directly proportional to the t_{re} (see the inset of Fig. S2A), indicated that pulsed potentiostatic electrodeposition is an easily controllable, distinct advantage over CRGO methods.

At the same time, according to Randles-Sevcik formula [37]: $i_{pa} = 2.69 \times 10^5 n^{3/2} A D_o^{1/2} c_o \nu^{1/2}$, where i_{pa} refers to the anodic peak current (A); n is the electron transfer number; A is the surface area of the electrode (cm^2); D_o is the diffusion coefficient (cm^2 s^{-1}); c_o is the concentration of $K_3[Fe(CN)_6]$ (mol L^{-1}) and ν is the scan rate (V s^{-1}). By exploring the redox peak current with scan rate, the average electroactive area of bare GCE, ERGO/GCE and PP-ERGO/GCE was calculated as 0.045, 0.068 and 0.090 cm^2, respectively. The results further indicated the preparation of the ERGO films by PPM could further enhance the effective area of the electrode surface.

3.4. Voltammetric behavior of sophoridine at PP-ERGO/GCE

Fig. 4 displays CVs of 1.0×10^{-4} mol L^{-1} sophoridine in 0.2 mol L^{-1} PBS (pH 7.5) at bare GCE (curve a), ERGO/GCE (curve b) and PP-ERGO/GCE (curve c), respectively. As can be seen, sophoridine showed electrochemical activation on all electrodes. At bare GCE, the electrochemical response of sophoridine was very weak and only a very small bulge was observed at 1.050 V. When the ERGO/GCE was applied, the oxidation peak cureents (i_p) was increased significantly and the peak potentials (E_p) was negatively shifted about 0.825 V, indicated that the RGO films could accelerated the electron transfer on the electrode surface to amplify the electrochemical signal due to its excellent electric conductivity and large specific surface area. In contrast, a distinct well-defined and more sensitive anodic peak appeared at the PP-ERGO/GCE under the same experimental condition, of which the i_p is about 9.8- and 1.4-fold higher than that of bare GCE and ERGO/GCE, respectively, and the E_p at the PP-ERGO/GCE is the lowest. The above results suggested that the preparation of ERGO films by PPM can provide an efficient interface and microenvironment for the electrochemical response of sophoridine.

For further investigating the redox properities of sophoridine at the PP-ERGO/GCE, successive CVs were performed. The inset of Fig. 4 shows CVs of the background (curve a) and successive CVs of 1.0×10^{-4} mol L^{-1} sophoridine in 0.2 mol L^{-1} PBS (pH 7.5) at PP-ERGO/GCE (curve b). It is obvious that the anodic peak current decreased obviously in the second scan compared with that of the first one, and gradually reduced with successive cyclic sweep. The reason may be that the oxidation product of sophoridine, which is non-electroactive, adhered to the electrode surface and hindered the access of sophoridine. At the same time, we found that if the electrodes were kept in PBS (pH = 7.5) in the absence of sophoridine for 3 min under constant stirring, and then CV was carried out in the solution with scan potential window of between 0.0 V to 1.0 V (vs SCE), until the peaks of sophoridine disappeared. Finally, the PP-ERGO/GCE surface will be restored to the initial state so that a new voltammogram then exhibits the same characteristics as those of the first cycle in the inset of Fig. 4. Therefore, in the following discussion, the peak current is taken from the first cycle.

To further elucidate the electrode reaction of sophoridine at PP-ERGO/GCE, the influence of potential scan rate (ν) on i_{pa} of 1.0×10^{-4} mol L^{-1} sophoridine was studied by CV in different sweep rates from 50 to 300 mV s^{-1}, see Fig. 5. The peak currents of sophoridine grow with the increasing of scan rates and there are good linear relationships between i_{pa} and ν, indicating the oxide process of sophoridine at PP-ERGO/GCE was an adsorption-controlled irreversible reaction. Furthermore, the oxidation peak potentials shift positively with the increasing scan rates. According to Laviron's theory [38], for an irreversible anodic reaction, the relationship between E_{pa} and ν is described as follows:

$$E_{pa}(V) = E^o - \frac{RT}{\alpha n F} \ln \frac{RTk_s}{\alpha n F} + \frac{RT}{\alpha n F} \ln \nu \quad (1)$$

Where E^o is the formal standard potential; α is the charge transfer coefficient; k_s is the apparent electron transfer rate constant; and others have their usual meaning. The inserted calibration plot in Fig. 5 highlighted a linear relationship between the variation of E_{pa} with the ν from 50 to 300 mV s^{-1} and a good linear equation was represented as E_{pa} (V) = 0.816 + 0.0271 lnν (mV s^{-1}) (R = 0.999). From the slope of the straight line of E_{pa} against lnν, αn = 0.94 could be obtained. As for a totally irreversible electrode process, the value of α is assumed as 0.5 [38], thus, the value of n is calculated to be 2 as a reasonable conjecture. In return, α was 0.47. Meanwhile, the value of k_s of 2.69 s^{-1} was calculated from the intercept of the straight line of E_{pa} vs. lnν. The value of E^o was determined to be 0.745 V from intercept of E_{pa} versus ν plot on the ordinate by extrapolating the line to be ν = 0.

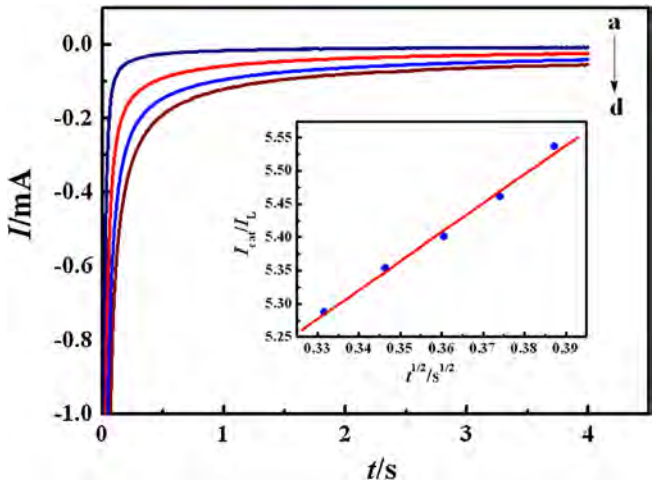

Fig. 6. Chronoamperograms of PP-ERGO/GCE in 0.2 mol L^{-1} PBS (pH = 7.5) containing (a) 0, (b) 50, (c) 100 and (d) 200 μmol L^{-1} sophoridine; inset shows the relationship of i_{cat}/i_L versus $t^{1/2}$ for 100 μmol L^{-1} sophoridine.

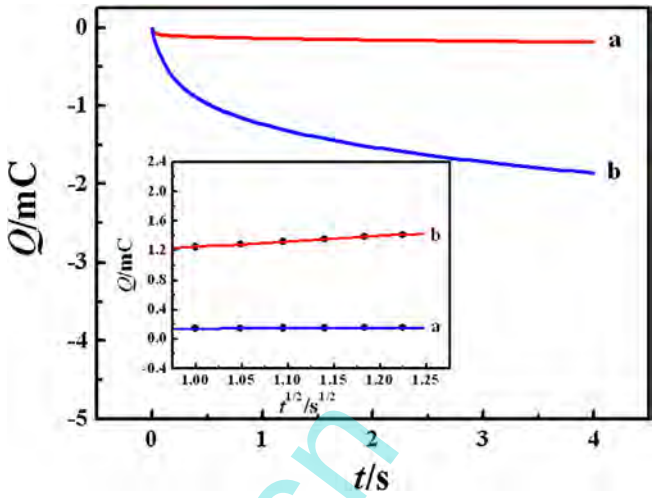

Fig. 7. Chronocoulometric curves of the background (curve a) and sophoridine (3.0×10^{-4} mol L^{-1}) (curve b) in 0.2 mol L^{-1} PBS (pH = 7.5) at the PP-ERGO/GCE; the inset is the corresponding $Q \sim t^{1/2}$ plots.

3.5. Chronoamperometry investigations

The evaluation of the catalytic rate constant (k_{cat}) was investigated by chronoamperometry. Fig. 6 shows chronoamperograms of PP-ERGO/GCE in 0.2 mol L^{-1} PBS (pH 7.5) in the absence (curve a) and presence (curves b-d) of sophoridine. The k_{cat} for the chemical reaction between sophoridine and PP-ERGO/GCE is determined according to the method described in the literature [39]:

$$\frac{i_{cat}}{i_L} = \pi^{1/2}(k_{cat}c_o t)^{1/2} \quad (2)$$

Where i_{cat} and i_L were the currents in the presence and the absence of sophoridine, respectively; k_{cat} was the catalytic rate constant (mol L^{-1} s^{-1}), c_o was the bulk concentration (mol L^{-1}) of sophoridine and t was the elapsed time (s). From the slope of the i_{cat}/i_L versus $t^{1/2}$ plot (see the inset of Fig. 6), the mean value of k_{cat} for the electrooxidation of sophoridine was calculated to be 6.04×10^4 mol L^{-1} s^{-1} when the concentration of sophoridine was 1.0×10^{-4} mol L^{-1}.

3.6. Chronocoulometry investigations

The chronocoulometry (CC) was employed to determine the saturating absorption capacity of sophoridine at PP-ERGO/GCE surface. The PP-ERGO/GCE was immersed in a sophoridine solution (3.0×10^{-4} mol L^{-1}) for several minutes to achieve saturated absorption. And then, a step potential from 0.0 V to 1.0 V was applied. $Q \sim t$ curve was recorded (Fig. 7, curve b) to calculate the saturated absorption capacity. For control, $Q \sim t$ curve was recorded in the blank solution too (Fig. 7, curve a). The corresponding $Q \sim t^{1/2}$ plots were also performed and shown as inset in Fig. 7. According to the formula given by Anson [40]:

$$Q = \frac{2nFAc(Dt)^{1/2}}{\pi^{1/2}} + Q_{dl} + Q_{ads} \quad (3)$$

Where Q_{dl} is the double-layer charge, and Q_{ads} is the Faradaic charge due to the oxidation of adsorbed sophoridine. Using Laviron's theory of $Q = nFA\Gamma^*$ (Γ^* is the maximum surface concentration of the surface-attached material (mol cm^{-2}), and A is the electrode geometric area (cm^2)) and intercept difference between curves a and b, a Γ^* value of 2.34×10^{-8} mol cm^{-2} was obtained.

3.7. Analytical applications and methods validation

3.7.1. Influence of supporting electrolyte and pH

The types of supporting electrolytes played a key role in the voltammetric responses of sophoridine. The current responses of 1.0×10^{-4} mol L^{-1} sophoridine were estimated in different supporting electrolytes such as H_2SO_4, NaOH, phosphate buffer, acetate buffer, Britton-Robinson and borate buffer solutions. The results showed that higher peak current and better peak shape could be achieved in PBS. Therefore, PBS was adopted.

For the variation of solution pH from 6.0 to 8.0, it was found that the E_{pa} shifted to lower values as the pH increased. The relationship between the E_{pa} and pH could be fitted into the regression equation: E_{pa} (V) = 1.182 – 0.057 pH (R= 0.997). The value of slope was 57 mV pH^{-1}, indicated that the same amounts of electrons and protons took part in the electrode reaction. Consequently, the oxidation mechanism for sophoridine can be written as Scheme 1, which is in accordance with the report [14]. Besides, the i_{pa} vary very little in the range; so solution pH of 7.5 was chosen in following experiments, which was close to human physiological pH.

3.7.2. Instrumental parameters

In order to obtain a much more sensitive detection, the square wave voltammetry (SWV) was employed in the determination of sophoridine. The optimum instrumental parameters (pulse-amplitude E_{sw}, frequency f) were studied for a 1.0×10^{-4} mol L^{-1} sophoridine solution. The results indicated the i_{pa} increased with the increasing of E_{sw} from 10 to 40 mV or f in the range of 10 - 40 Hz, but the peak potential shifted to more positive values, and

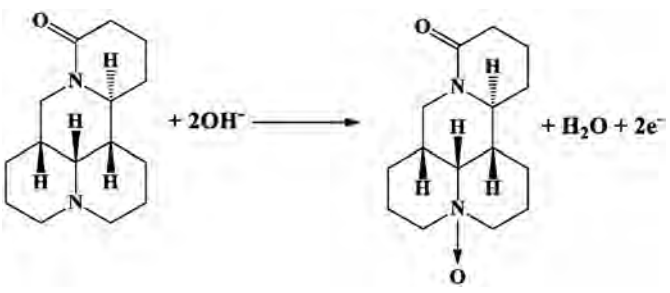

Scheme 1. Oxidation mechanism of sophoridine at PP-ERGO/GCE.

Table 1
Application of the SWASV method to the determination of sophoridine in spiked urine samples.

Sample	Original Found	Added (1.0 × 10−6 mol L−1)	Total Found [b] (1.0 × 10−6 mol L−1)	R.S.D. (%)	Recovery (%)
1	ND[a]	1.00	1.04	3.5	104.0
2	ND[a]	4.00	4.19	3.7	104.8
3	ND[a]	7.00	6.89	4.1	98.4
4	ND[a]	10.00	9.59	3.1	95.9

[a] ND: None detected
[b] Average of three determinations

the peak changed unshapely. So 30 mV were chosen as the optimum amplitude and 25 Hz were chosen as the optimum frequency.

3.7.3. Accumulation conditions

For consideration of the adsorption of sophoridine on the PP-ERGO/GCE surface, SWV technique coupled with accumulation procedure was used for study. With an increase in accumulation time (t_{acc}), the i_{pa} increased; but electrode renewal was also more difficult. Moreover, the accumulation potential (E_{acc}) had a little effect on the i_{pa}. So the t_{acc} of 120 s under open circuit was used for further studies.

3.7.4. Calibration curve, detection limit, reproducibility and stability

Series concentrations of sophoridine standard solutions were detected under the optimized working conditions described above. Fig. 8 displayed the response of different concentration of sophoridine by square wave adsorptive stripping voltammetry (SWASV). A linear relationship could be established between i_{pa} and the concentration of sophoridine in the range of $8.0 \times 10^{-7} \sim 1.0 \times 10^{-4}$ mol L^{-1}, see the inset of Fig. 8. The linear regression equation and correlation coefficient are:

$$i_{pa} = 5.214 + 0.540 \times 10^{6} c (R = 0.999)$$

where i_{pa} was the oxidation peak current in μA and c was the concentration of sophoridine in mol L^{-1}. Standard deviations (SD) for the slope and intercept of the calibration curve were 0.00102 and 0.0404, respectively. Based on the signal-to-noise ratio of 3 (S/N) [41], the detection limit was obtained as 2.0×10^{-7} mol L^{-1}. These values confirmed the sensitivity of the proposed method for the determination of sophoridine. To estimate the reproducibility of the proposed electrode, the R.S.D. of five times successful measurement the peak current of 2.0×10^{-5} mol L^{-1} sophoridine was calculated to be 3.6%, which demonstrated the good reproducibility of the proposed electrode. The PP-ERGO/GCE can be stored about 4 weeks and the decrease of the response was got as 5.4%, which indicated that PP-ERGO/GCE had good stability.

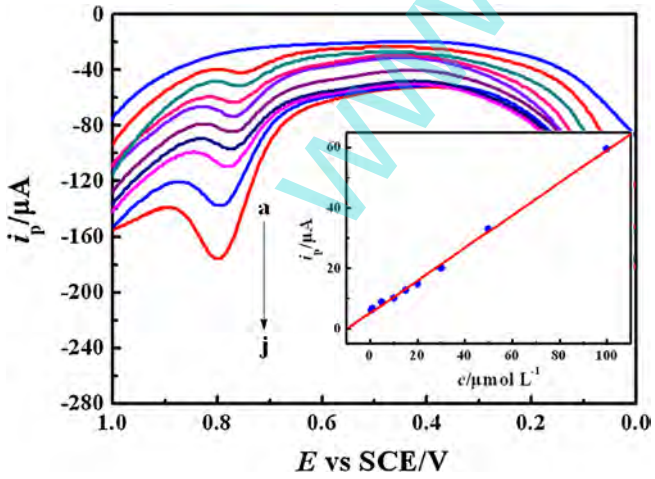

Fig. 8. Square wave anodic stripping voltammograms and their associated calibration plot (insert) for increasing concentrations of sophoridine at the PP-ERGO/GCE under optimum conditions; sophoridine concentration: a) 0.0 mol L^{-1}, b) 8.0×10^{-7} mol L^{-1}, c) 1.0×10^{-6} mol L^{-1}, d) 5.0×10^{-6} mol L^{-1}, e) 1.0×10^{-5} mol L^{-1}, f) 1.5×10^{-5} mol L^{-1}, g) 2.0×10^{-5} mol L^{-1}, h) 3.0×10^{-5} mol L^{-1}, i) 5.0×10^{-5} mol L^{-1}, j) 1.0×10^{-4} mol L^{-1}.

The proposed PP-ERGO/GCE for sophoridine determination was compared with other method reported and the results were listed in Table S1. It is clear that the proposed electrodes can achieve wider linear concentration ranges and lower detection limits. Besides, this research suggests that the synthesis of ERGO by PPM as voltammetric sensors might be a very promising direction in trace analysis of electrochemistry.

3.7.5. Interference studies

For the possible analytical application of the proposed method, various possible interfering species were evaluated, with a fixed sophoridine concentration of 5.0×10^{-5} mol L^{-1}. The selected interferents were some species that were posible exist in human urine samples, and the tolerance limit for a foreign species was taken as the largest amount yielding a relative error < ± 5% for the determination of sophoridine. The experiment results showed that no interference could be observed for the following organic compounds: glucose (500), citric acid (500), glutamic acid (500), oxalic acid (500), ascorbic acid (5), uric acid (5) and norepinephrine (3), where the data in brackets denote the molar ratio of interfering compound to sophoridine. At the same time, the inorganic species, such as Ca^{2+}, Zn^{2+}, NH_4^+, Cl^-, SO_4^{2-}, $PO_4^{3-}$and Ac^- did not interfere. The results indicate the present method was adequate for the determination of sophoridine in real samples.

3.8. Determination of sophoridine in spiked urine samples

In order to evaluate the validity of the proposed method, it was employed to determine sophoridine in spiked urine samples. There was no distinct signal of sophoridine was observed in the original urine sample. But, a new wave was found at potential about 0.46 V, and we do not know what it is. But it does not distinctly affect to the peak intensity i_p and the peak potential E_p of the oxidation of sophoridine. For evaluating the veracity, some sophoridine standard solution was added in a urine sample before analysis. The direct determination of sophoridine in spiked urine samples was found to be possible by employing a high dilution of the sample with the supporting electrolyte. The determination of sophoridine concentration was performed by the calibration curve method. The results of determination are listed in Table 1. The mean recovery of sophoridine was 100.8%.

4. Conclusions

We have demonstrated pulsed potentiostatic method to prepare ERGO films for the sensitive detection of sophoridine. The ERGO films modified electrode showed enhanced electron transfer properties and high resolution capacity to the sophoridine, superior to that of potentiostatic method. Wide linear concentration

ranges, low detection limits, and excellent reproducibility and stability were achieved on the modified electrode, indicating the prepared ERGO films by pulsed potentiostatic method might be a very promising platform for analytical sensing.

Acknowledgements

The authors would like to thank the financial supports from the National Science Foundation of China (No. 21172054, 21275132), and the Joint Funds of the National Science Foundation of China - Henan province people's Government (No. U1304213).

Appendix A. Supplementary data

Supplementary data associated with this article can be found, in the online version, at http://dx.doi.org/10.1016/j.electacta.2014.07.018.

References

[1] B.G. Zhao, Studies on the alkaloids of Sophora alopecuroides, Acta Pharmaceutica Sinica 15 (1980) 182.
[2] H.M. Zhang, H.Q. Li, Anti-arrhythmic effects of sophoridine and oxysophoridine, Acta Pharmacologica Sinica 20 (1999) 517–520.
[3] Y.Y. Zhang, H.Y. Zhu, G. Ye, C.G. Huang, Y.Z. Yang, R.Z. Chen, Y. Yu, X.L. Cui, Antiviral effects of sophoridine against coxsackievirus B3 and its pharmacokinetics in rats, Life Sciences 78 (2006) 1998–2001.
[4] S.C. Tao, J.Z. Wang, Pharmacological action of alkaloids from Sophora alopecuroidesl, Chinese Pharmaceutical Journal 27 (1992) 201–204.
[5] Z. Lin, C.F. Huang, X.S. Liu, J.K. Jiang, In Vitro Anti-Tumour Activities of Quinolizidine Alkaloids Derived from Sophora Flavescens Ait, Basic & Clinical Pharmacology & Toxicology 108 (2011) 304–309.
[6] X. Li, W.L. Zhao, J.D. Jiang, K.H. Ren, N.-N. Du, Y.B. Li, Y.X. Wang, C.W. Bi, R.G. Shao, D.Q. Song, Synthesis, structure-activity relationship and biological evaluation of anticancer activity for novel N-substituted sophoridinic acid derivatives, Bioorganic & Medicinal Chemistry Letters 21 (2011) 5251–5254.
[7] Y.H. Wei, X.A. Wu, X.F. Liu, J.Y. Luo, A rapid reversed phase high-performance liquid chromatographic method for determination of sophoridine in rat plasma and its application to pharmacokinetics studies, Journal of Chromatography B-Analytical Technologies in the Biomedical and Life Sciences 843 (2006) 10–14.
[8] Y.J. Wu, J.J. Chen, Y.Y. Cheng, A sensitive and specific HPLC-MS method for the determination of sophoridine, sophocarpine and matrine in rabbit plasma, Analytical and Bioanalytical Chemistry 382 (2005) 1595–1600.
[9] N. Chen, Z. Han, L. Luan, Y. Wu, Simultaneous Determination of Four Alkaloids in Gan-Yan-Ling Injection by GC-MS, Chromatographia 70 (2009) 299–303.
[10] J.Z. Song, H.X. Xu, S.J. Tian, P.P.H. But, Determination of quinolizidine alkaloids in traditional Chinese herbal drugs by nonaqueous capillary electrophoresis, Journal of Chromatography A 857 (1999) 303–311.
[11] X. Chen, C.Q. Yi, M.J. Li, X. Lu, Z. Li, P.W. Li, X.R. Wang, Determination of sophoridine and related lupin alkaloids using tris(2,2 '-bipyridine)ruthenium electrogenerated chemiluminescence, Analytica Chimica Acta 466 (2002) 79–86.
[12] (!!! INVALID CITATION !!!).
[13] Y.F. Li, L.N. Zou, G. Song, K.J. Li, B.X. Ye, Electrochemical behavior of sophoridine at a new amperometric sensor based on L-Theanine modified electrode and its sensitive determination, Journal of Electroanalytical Chemistry 709 (2013) 1–9.
[14] H. Liu, W.P. Wu, X.H. Zhu, B.X. Ye, Investigation on electrochemical reaction mechanism of sophoridine and its electroanalytical application, Journal of Zhengzhou Universit (Medical Sciences) 45 (2010) 495–498.
[15] M. Zhou, J. Ding, L.P. Guo, Q.K. Shang, Electrochemical behavior of L-cysteine and its detection at ordered mesoporous carbon-modified glassy carbon electrode, Analytical Chemistry 79 (2007) 5328–5335.
[16] L.N. Wu, X.J. Zhang, H.X. Ju, Amperometric glucose sensor based on catalytic reduction of dissolved oxygen at soluble carbon nanofiber, Biosensors and Bioelectronics 23 (2007) 479–484.
[17] C.E. Banks, T.J. Davies, G.G. Wildgoose, R.G. Compton, Electrocatalysis at graphite and carbon nanotube modified electrodes: edge-plane sites and tube ends are the reactive sites, Chemical Communications (2005) 829–841.
[18] A.K. Geim, Graphene: Status and Prospects, Science 324 (2009) 1530–1534.
[19] A.K. Geim, K.S. Novoselov, The rise of graphene, Nature Materials 6 (2007) 183–191.
[20] J.L. Zhang, H.J. Yang, G.X. Shen, P. Cheng, J.Y. Zhang, S.W. Guo, Reduction of graphene oxide via L-ascorbic acid, Chemical Communications 46 (2010) 1112–1114.
[21] S. Stankovich, D.A. Dikin, R.D. Piner, K.A. Kohlhaas, A. Kleinhammes, Y. Jia, Y. Wu, S.T. Nguyen, R.S. Ruoff, Synthesis of graphene-based nanosheets via chemical reduction of exfoliated graphite oxide, Carbon 45 (2007) 1558–1565.
[22] G.K. Ramesha, S. Sampath, Electrochemical Reduction of Oriented Graphene Oxide Films: An in Situ Raman Spectroelectrochemical Study, Journal of Physical Chemistry C 113 (2009) 7985–7989.
[23] H.L. Guo, X.F. Wang, Q.Y. Qian, F.B. Wang, X.H. Xia, A Green Approach to the Synthesis of Graphene Nanosheets, ACS Nano 3 (2009) 2653–2659.
[24] Y.Y. Shao, J. Wang, M. Engelhard, C.M. Wang, Y.H. Lin, Facile and controllable electrochemical reduction of graphene oxide and its applications, Journal of Materials Chemistry 20 (2010) 743–748.
[25] J.F. Ping, Y.X. Wang, K. Fan, J. Wu, Y.B. Ying, Direct electrochemical reduction of graphene oxide on ionic liquid doped screen-printed electrode and its electrochemical biosensing application, Biosensors and Bioelectronics 28 (2011) 204–209.
[26] Z.J. Wang, X.Z. Zhou, J. Zhang, F. Boey, H. Zhang, Direct Electrochemical Reduction of Single-Layer Graphene Oxide and Subsequent Functionalization with Glucose Oxidase, The Journal of Physical Chemistry C 113 (2009) 14071–14075.
[27] Z.J. Wang, S.X. Wu, J. Zhang, P. Chen, G.C. Yang, X.Z. Zhou, Q.C. Zhang, Q.Y. Yan, H. Zhang, Comparative studies on single-layer reduced graphene oxide films obtained by electrochemical reduction and hydrazine vapor reduction, Nanoscale Research Letters 7 (2012) 1–7.
[28] S. Wu, F.F. Huang, X.Q. Lan, X.Y. Wang, J.M. Wang, C.G. Meng, Electrochemically reduced graphene oxide and Nafion nanocomposite for ultralow potential detection of organophosphate pesticide, Sensors and Actuators B-Chemical 177 (2013) 724–729.
[29] Y. Kong, X. Ren, Z. Huo, G. Wang, Y. Tao, C. Yao, Electrochemical detection of pyrosine with electrochemically reduced graphene oxide modified glassy carbon electrode, European Food Research and Technology 236 (2013) 955–961.
[30] L.Y. Chen, Y.H. Tang, K. Wang, C.B. Liu, S.L. Luo, Direct electrodeposition of reduced graphene oxide on glassy carbon electrode and its electrochemical application, Electrochemistry Communications 13 (2011) 133–137.
[31] V. Mani, B. Devadas, S.M. Chen, Direct electrochemistry of glucose oxidase at electrochemically reduced graphene oxide-multiwalled carbon nanotubes hybrid material modified electrode for glucose biosensor, Biosensors & Bioelectronics 41 (2013) 309–315.
[32] J. Yang, S. Gunasekaran, Electrochemically reduced graphene oxide sheets for use in high performance supercapacitors, Carbon 51 (2013) 36–44.
[33] A. Davies, P. Audette, B. Farrow, F. Hassan, Z.W. Chen, J.Y. Choi, A.P. Yu, Graphene-Based Flexible Supercapacitors: Pulse-Electropolymerization of Polypyrrole on Free-Standing Graphene Films, The Journal of Physical Chemistry C 115 (2011) 17612–17620.
[34] W.S. Hummers, R.E. Offeman, Preparation of Graphitic Oxide, Journal of the American Chemical Society 80 (1958) 1339.
[35] S. Park, J. An, R.D. Piner, I. Jung, D. Yang, A. Velamakanni, S.T. Nguyen, R.S. Ruoff, Aqueous Suspension and Characterization of Chemically Modified Graphene Sheets, Chemistry of Materials 20 (2008) 6592–6594.
[36] M.S. Chandrasekar, M. Pushpavanam, Pulse and pulse reverse plating—Conceptual, advantages and applications, Electrochimica Acta 53 (2008) 3313–3322.
[37] A.J. Bard, L.R. Faulkner, Electrochemical Methods, Fundamentals and Applications, 2nd ed, Wiley, New York, 2001.
[38] E. Laviron, General expression of the linear potential sweep voltammogram in the case of diffusionless electrochemical systems, Journal of Electroanalytical Chemistry 101 (1979) 19–28.
[39] M.H. Pournaghi-Azar, R. Sabzi, Electrochemical characteristics of a cobalt pentacyanonitrosylferrate film on a modified glassy carbon electrode and its catalytic effect on the electrooxidation of hydrazine, Journal of Electroanalytical Chemistry 543 (2003) 115–125.
[40] F.C. Anson, Application of Potentiostatic Current Integration to the Study of the Adsorption of Cobalt(III)-(Ethylenedinitrilo(tetraacetate) on Mercury Electrodes, Analytical Chemistry 36 (1964) 932–934.
[41] J.N. Miller, J.C. Miller, Statistics and Chemometrics for Analytical Chemistry, fourth ed., Pearson Education Limited, London, 2000.